17th Australasian Fluid Mechanics Conference
Auckland, New Zealand
5-9 December 2010

Control of Convective Rolls by Spatially Distributed Wall Heating

M. Z. Hossain and J. M. Floryan

Department of Mechanical and Materials Engineering
The University Of Western Ontario, London, ON, N6A 5B9, Canada

Abstract

Conditions leading to the emergence of convective roll instability have been identified by linear instability analysis of a stationary fluid in a slot subject to spatially distributed heating. It is found that for moderate heating wave numbers the pattern of instability is generally locked-in with the pattern of heating by a sub-harmonic relation, and for large heating wave numbers, the critical wave number of the rolls has the same value as the critical wave number of the rolls for uniform heating. Four different types of flow responses are observed depending on the Prandtl number of fluid.

Introduction

Thermal convection plays an important role in many industrial and engineering applications. A layer of fluid heated from below, widely known as Rayleigh-Benard convection (RBC), characterizes an idealized version of thermal convection. Various forms of the motion associated with this convection, i.e., patterns, have been observed. A good summary is given by Bodenschatz et al. [1]. Very few analyses focused on RBC with spatial variation of temperature are available. Mancho et al [4] studied convection in a container with the upper surface open to the air and heated from below using a Gaussian-like temperature distribution. They used silicon oil with Prandtl number Pr = 40.32 as the working fluid. Rossby [7] carried out numerical experiments on convection in a insulated square container whose bottom wall was exposed either to linear or to non-linear temperature distributions and contained fluids with Pr = 1-100. Mullarney et al. [5] performed both laboratory and numerical experiments with the convective circulation that develops in a long channel driven by heating and cooling through opposite halves of the horizontal base. Wang and Huang [8] studied experimentally circulation driven by horizontal differential heating in a tank filled with salt water. They maintained linear temperature profile either along the lower or the upper boundary. Similar study was done by Lyubimova et al. [3], but they used horizontal channel with rectangular-cross section. Natarajan et al. [6] performed a parametric study using computer simulations of natural convection inside a trapezoidal cavity with the bottom wall either uniformly and non-uniformly heated while the two vertical walls were maintained at constant temperatures and the top wall was insulated. They considered Pr = 0.07-100.

The present work deals with the analysis of convection control strategy based on the use of spatially distributed wall heating of a slot containing fluid. The heating is such that both walls have the 'same' average temperatures. The spatial distribution of heating is controlled through imposition of the heating wave number α. The analysis is carried out for Prandtl numbers in the range from 10^{-2} to 10^{3} and thus covers the range of all possible practical applications [9]. Detailed results are presented for heating patterns described by a single Fourier mode.

Problem Formulation

Consider steady motion of fluid contained in a slot between two plane parallel plates extending to $\pm\infty$ in the x-direction and placed at a distance 2h apart from each other with the gravitational acceleration g acting in the negative y-direction, as shown in Fig. 1. Motion of the fluid is driven by buoyancy forces resulting in the formation of convective rolls. The fluid is incompressible, Newtonian, with thermal conductivity k, specific heat per unit mass c, thermal diffusivity $\kappa=k/\rho c$, kinematic viscosity ν, dynamic viscosity μ, thermal expansion coefficient Γ and variations of the density ρ following the Boussinesq approximation. All material properties need to be evaluated at the reference temperature defined below. The temperature of the upper wall (θ_U) is kept constant and the lower plate is subject to a distributed heating with temperature of the lower (θ_L) wall described by the following relations

$$\theta_L(x)=\sum_{n=-\infty}^{n=+\infty}\theta_L^{(n)}e^{in\alpha x} \quad . \tag{1}$$

where α stands for the wave number of the heating, θ denotes the relative temperature, i.e. $\theta=T-T_{ref}$, T denotes the temperature and T_{ref} denotes the reference temperature. The reality condition has the form $\theta^{(n)}=\theta^{(-n)*}$ where stars denote complex conjugates. The wavelength of the heating is denoted as $\lambda_x=2\pi/\alpha$. It is assumed that the mean temperatures of the both plates are equal, i.e., $\theta_U=\theta_L^{(0)}=0$.

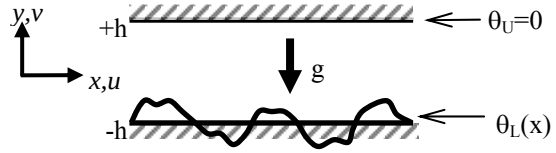

Figure 1: Fluid layer subject to spatially distributed thermal forcing.

The temperature field is represented as a sum of conductive field θ_0 and deviations θ_1 associated with convective effects. We introduce two temperature scales, i.e., we use the amplitude of the temperature variations along the plates as the conductive temperature scale T_d and $T_v=T_d\nu/\kappa$ as the convective temperature scale, where $T_v/T_d=Pr$, with $Pr=\nu/\kappa$ denoting the Prandtl number. We select half distance h between the plates as the length scale, $U_v=\nu/h$ as the (convective) velocity scale and $P_v=\rho U_v^2$ as the (dynamic) pressure scale. The complete dimensionless temperature is scaled using the convective scale, i.e.,

$$\theta(x,y)=Pr^{-1}\theta_0(x,y)+\theta_1(x,y) \tag{2}$$

where the conductive temperature is a solution of the following problem

$$\frac{\partial^2\theta_0}{\partial x^2}+\frac{\partial^2\theta_0}{\partial y^2}=0\,,\quad \theta_0(x,-1)=\sum_{n=-\infty}^{n=+\infty}\theta_L^{(n)}e^{in\alpha x}\,, \tag{3}$$

and has the form

$$\theta_0(x,y)=\theta_L^{(n)}\left[-\frac{\sinh(n\alpha y)}{2\sinh(n\alpha)}+\frac{\cosh(n\alpha y)}{2\cosh(n\alpha)}\right]e^{in\alpha x}, \qquad (4)$$

with $\theta_0^{(0)}(y)=0$. The dimensionless field equations describing motion of the fluid and the resulting changes in the temperature field have the form

$$\frac{\partial\psi}{\partial y}\frac{\partial}{\partial x}\left(\nabla^2\psi\right)-\frac{\partial\psi}{\partial x}\frac{\partial}{\partial y}\left(\nabla^2\psi\right)=\nabla^4\psi-Ra\frac{\partial\theta_1}{\partial x}-Ra\,Pr^{-1}\frac{\partial\theta_0}{\partial x}, \quad (5a)$$

$$Pr\left(\frac{\partial\psi}{\partial y}\frac{\partial\theta_1}{\partial x}-\frac{\partial\psi}{\partial x}\frac{\partial\theta_1}{\partial y}\right)+\frac{\partial\psi}{\partial y}\frac{\partial\theta_0}{\partial x}-\frac{\partial\psi}{\partial x}\frac{\partial\theta_0}{\partial y}=\nabla^2\theta_1 \qquad (5b)$$

where **v** = (u,v) denotes the velocity vector, p stands for the pressure, $Ra=g\Gamma h^3T_d/\nu\kappa$ is the Rayleigh number, ∇^2 denotes the Laplace operator, dissipation effects have been neglected in the energy equation and the stream function $\psi(x,y)$ is defined in the usual manner, i.e., $u=\partial\psi/\partial y$, $v=-\partial\psi/\partial x$. Introduction of stream function permits elimination of pressure from the field equations. The boundary conditions take the form

$$u(\pm1)=0, \quad v(\pm1)=0, \quad \theta_1(\pm1)=0 \qquad (6)$$

The solution is assumed in the form of Fourier expansions, i.e.,

$$\psi=\sum_{n=-\infty}^{n=+\infty}\varphi^{(n)}(y)e^{in\alpha x}, \ \theta_1=\sum_{n=-\infty}^{n=+\infty}\phi^{(n)}(y)e^{in\alpha x}. \qquad (7)$$

Substitution of equation (7) into (5) and separation of Fourier components result in a following system of ordinary differential equations

$$D_n^2\varphi^{(n)}-in\alpha Ra\phi^{(n)}= i\alpha\sum_{m=-\infty}^{m=+\infty}\left[D\varphi^{(n-m)}mD_m\varphi^{(n)}-(n-m)\varphi^{(n-m)}D_m\left(D\varphi^{(n)}\right)\right], \qquad (8a)$$

$$D_n\phi^{(n)}=i\alpha\sum_{m=-\infty}^{m=+\infty}\left[(n-m)\left(\theta_0^{(n-m)}+Pr\,\phi^{(n-m)}\right)D\varphi^{(n)} -m\varphi^{(n)}D\left(\theta_0^{(n-m)}+Pr\,\phi^{(n-m)}\right)\right] \qquad (8b)$$

where $-\infty<n<+\infty$, $D=d/dy$ and $D_n=D^2-n^2\alpha^2$. The required boundary conditions have the form

$$\varphi^{(n)}(\pm1)=0, \ D\varphi^{(n)}(\pm1)=0, \ \phi^{(n)}(\pm1)=0 \ \text{ for } -\infty<n<+\infty. \qquad (9a\text{-}c)$$

The system (8) together with the boundary conditions (9) needs to be solved numerically. The solution method uses variable-step-size finite-difference discretization based on the Simpson method with deferred correction [2] with the resulting algebraic system being solved using a simplified Newton (chord) method with residual control. The selection of the number and distribution of grid points is done automatically so that the specified error bounds are met. The number of Fourier modes used in the solution was selected through numerical experiments so that the flow quantities of interest were determined with at least six digits accuracy.

After the obtaining the solution of the steady flow, the linear stability analysis of the above flow is considered. The analysis begins with the governing equations expressed in terms of stream function and temperature. Unsteady, two-dimensional disturbances are super-imposed on the mean part and the system is linearized. The disturbance stream function and temperature fields can be expressed as

$$\psi_3(x,y,t)=\sum_{m=-\infty}^{m=+\infty}\varphi_3^{(m)}(y)e^{i[(\delta+m\alpha)x-\sigma t]}+c.c. \qquad (10a)$$

$$\theta_3(x,y,t)=\sum_{m=-\infty}^{m=+\infty}\phi_3^{(m)}(y)e^{i[(\delta+m\alpha)x-\sigma t]}+c.c. \qquad (10b)$$

where δ is the x-wave number of disturbances, σ denotes the complex amplification whose real part represents the frequency of disturbances and imaginary part denotes the growth rate of disturbances, and c.c. means complex conjugate. Substituting Eq. (10) into the disturbance equations and separation of the Fourier components results, after a lengthy algebra, in a system of linear ordinary differential equations in the form,

$$S^{(m)}\varphi_3^{(m)}-it_m\theta_3^{(m)}=i\sum_{n=-\infty}^{n=+\infty}\left[t_nD\varphi_2^{(m-n)}H^{(n)}\varphi_3^{(n)} +(m-n)\alpha G^{(m-n)}\varphi_2^{(m-n)}D\varphi_3^{(n)} -(m-n)\alpha\varphi_2^{(m-n)}H^{(n)}D\varphi_3^{(n)}-t_nG^{(m-n)}D\varphi_2^{(m-n)}\varphi_3^{(n)}\right] \qquad (11a)$$

$$P^{(m)}\theta_3^{(m)}=i\,Pr\sum_{n=-\infty}^{n=+\infty}\left[t_nD\varphi_2^{(m-n)}\theta_3^{(n)}+(m-n)\alpha\theta_2^{(m-n)}D\varphi_3^{(n)} -(m-n)\alpha\varphi_2^{(m-n)}D\theta_3^{(n)}-t_nD\theta_2^{(m-n)}\varphi_3^{(n)}\right] \qquad (11b)$$

where

$$S^{(m)}=\left(D^2-t_m^2\right)^2+i\sigma\left(D^2-t_m^2\right), \ H^{(n)}=D^2-t_n^2,$$
$$P^{(m)}=D^2-t_m^2+i\,Pr\,\sigma, \ G^{(m-n)}=D^2-(m-n)^2\alpha^2,$$
$$t_m=\delta+m\alpha, \ t_n=\delta+n\alpha.$$

The reader may note that subscripts 3 and 2 in the above expressions refer to the disturbance and mean flow quantities, respectively.

Equations (11a-b) together with the homogeneous boundary conditions have nontrivial solution only for certain combinations of parameters Pr, Ra, δ, α and σ. The required dispersion relation has to be determined numerically through solution of the relevant eigenvalue problem. The system is posed as an eigenvalue problem for σ. Equations (11a-b) are discretized with spectral accuracy using Chebyshev Collocation method. The eigenvalues obtained are further refined using 'inverse iteration' technique. For the purpose of eigenvalue tracking a classical 'Newton-Raphson' and 'inverse iteration' search procedures have been used. A reasonable guess for the unknown eigenvalue is essential for the convergence of the 'Newton-Raphson' search routine, but the 'inverse iteration' routine is quite flexible.

Discussion

We focus our attention on the simplest reference case where the temperature distribution along the bottom wall is expressed by one Fourier mode, i.e., $\theta_L=0.5\cos(\alpha x)$. Various test calculations and scans through the parameter space suggest that there exist only stationary disturbances, i.e., Real(σ)=0. We shall refer to such disturbances as rolls. No travelling wave disturbances have been found. We have examined this roll instability for Prandtl numbers varying from 10^3 to 10^{-2}. We shall begin description of the critical stability conditions, of the structure of the disturbance motion and how the instability responds to changes in the spatial pattern of heating by considering at first fluid with the Prandtl number Pr=7. Such value of Pr closely approximates properties of water. It also serves as an example of large Pr fluids as differences found in the stability characteristics for fluids with Pr = 7 and Pr = 100 are rather small.

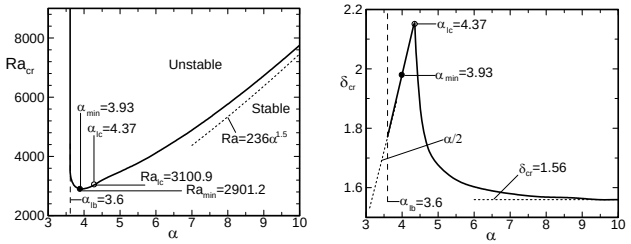

Figure 2. Variations of the critical Rayleigh number Ra_{cr} (left) and the critical disturbance wave number δ_{cr} (right) as functions of the heating wave number α for Pr = 7.

Critical instability (the most dangerous disturbances) diagrams are shown in Fig. 2 as a function of the heating wave number α. The intensity of the heating required to induce roll instability, as measured by Ra_{cr}, is a strong function of the heating wave number α. The lowest value of Ra_{cr} is $Ra_{min} = 2901.2$ and it occurs for $\alpha = \alpha_{min} = 3.93$. The fluid is rapidly stabilized when α decreases below this value and, as a matter of fact, this instability does not occur when $\alpha < \alpha_{lb} = 3.6$ in the range of Ra considered in this analysis. When α increases above α_{min}, the Ra_{cr} gradually increases, which implies that higher intensity of heating is required to induce the instability. When α is big enough, the increase of Ra_{cr} follows asymptote in the form $Ra_{cr} = 236\ \alpha^{1.5}$ (Fig.2). When $\alpha < \alpha_{lc} = 4.37$ the heating pattern and the disturbance pattern are locked-in according to the relation $\delta_{cr} = \alpha/2$. When $\alpha > \alpha_{lc}$, the lock-in is broken and there is no obvious relation between the heating pattern and the disturbance pattern. When $\alpha \to \infty$, the critical wave number δ_{cr} reaches to the asymptotic value $\delta_{cr} = 1.56$, which is the same as found in the case of the classical instability of fluid uniformly heated from below. The disturbance pattern for the lock-in situation is illustrated in Fig.3 for $\alpha = 4.3$, which just below the lock-in value of $\alpha_{lc} = 4.37$. The sub-harmonic relation between the basic state pattern and the disturbance pattern is clearly visible.

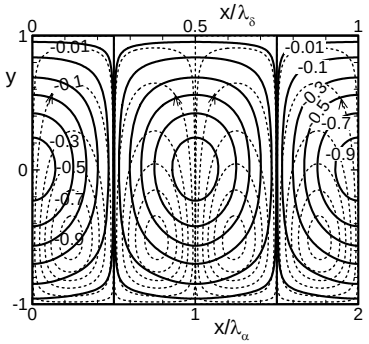

Figure 3. Disturbance streamlines for the heating wave number $\alpha = 4.3$ and the Rayleigh number $Ra_{cr} = 3048.4$ for the fluid with the Prandtl number Pr = 7. Dotted lines for the meanflow, and solid lines for disturbances.

Now, we shall discuss the case of Pr=0.04. This particular value of the Prandtl number has been selected to represent low Pr fluids and is typical for liquid metals. Critical instability diagrams are displayed in Fig. 4 and demonstrate qualitatively different responses of the system. Two critical branches have been identified. The first one describes system response for smaller heating wave numbers, i.e., $\alpha < \alpha_s = 8.76$, where rolls that are locked-in with the heating pattern according to a sub-harmonic relation in the form $\delta_{cr} = \alpha/2$. The minimum value of Ra for this branch is $Ra_{min,1} = 1087.7$ and it occurs at $\alpha_{min,1} = 4.04$. The rolls are fully stabilized for $\alpha < \alpha_{lb} = 3.8$ for the range of Ra considered and the critical Rayleigh number increases as $Ra_{cr} = 9.8\alpha^{3.1}$ for $\alpha \to \infty$. The second branch describes critical conditions for larger heating wave numbers, i.e., $\alpha > \alpha_s = 8.76$, where the rolls are not locked-in with the heating. The minimum value of Ra for this branch is $Ra_{min,2} = 6289.4$, it corresponds to the minimum value of the disturbance wave number $\delta_{cr} = \delta_{min,2} = 0.96$ and it occurs at $\alpha_{min,2} = 9.8$. The Rayleigh number increases as $Ra_{cr} = 236\alpha^{1.5}$ and $\delta_{cr} \to 1.56$ when $\alpha \to \infty$. The asymptotic behavior is the same as the case of Pr=7. Two different disturbance structures co-exist at the onset of instability for the heating wave number $\alpha = \alpha_s = 8.76$, i.e., the locked-in structure characterized by $\delta_{s1} = 4.38$ and the unlocked structure described by $\delta_{s2} = 1.61$.

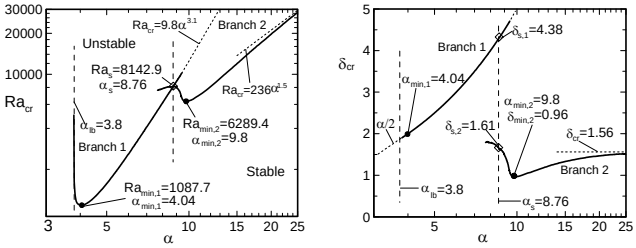

Figure 4. Variations of the critical Rayleigh number Ra_{cr} (left) and the critical disturbance wave number δ_{cr} (right) as functions of the heating wave number α for Pr = 0.04.

The disturbance velocity and temperature fields for the locked-in patterns (branch 1) at the onset of instability are illustrated in Fig.5 for conditions corresponding to $\alpha_{min,1} = 4.04$ and in Fig.6 for conditions corresponding to the intersection of both branches, i.e., $\alpha_s = 8.76$. The sub-harmonic relation between the primary convection and the disturbance field is clearly visible. The emergence of the second layer of rolls at the top of the slot for larger heating wave numbers is observed.

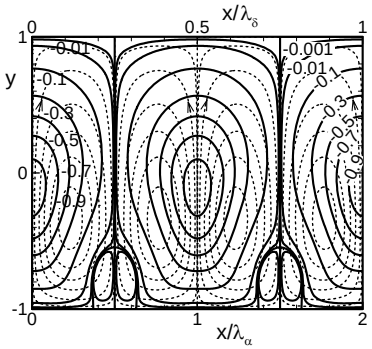

Figure 5. Disturbance streamlines for branch one of the instability for the heating wave number $\alpha = \alpha_{min,1} = 4.04$ and the Rayleigh number $Ra_{cr} = Ra_{min,1} = 1087.7$ for the fluid with the Prandtl number Pr = 0.04. Dotted lines for the meanflow, and solid lines for disturbances.

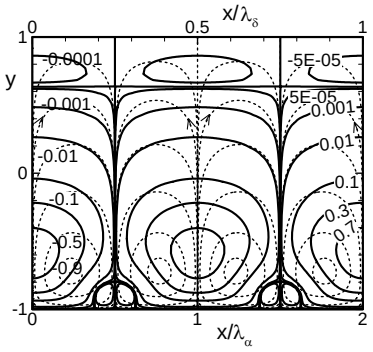

Figure 6. Disturbance streamlines for branch one of the instability for conditions corresponding to the intersection of both branches, i.e., for the heating wave number $\alpha = \alpha_s = 8.76$ and the Rayleigh number $Ra_{cr} = Ra_s = 8142.9$ for the fluid with the Prandtl number Pr = 0.04. Dotted lines for the meanflow, and solid lines for disturbances.

Disturbance pattern corresponding to the intersection of both branches, i.e., $\alpha_s = 8.76$, corresponding to branch 2 is displayed in Fig.7. This pattern is markedly different from the branch 1 pattern at the intersection point displayed in Fig. 6 and its form is difficult to characterize.

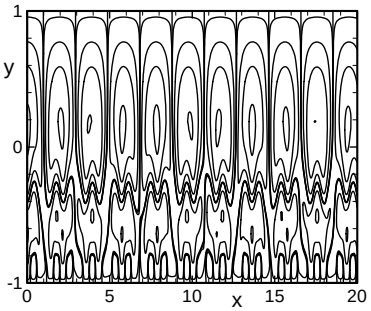

Figure 7. Disturbance flow field for branch 2 of the instability for conditions corresponding to the intersection of both branches, i.e., for the heating wave number $\alpha = \alpha_s = 8.76$, the Rayleigh number $Ra_{cr} = Ra_s = 8142.9$ and the critical disturbance wave number $\delta_{s2} = 1.61$ for the fluid with the Prandtl number Pr = 0.04.

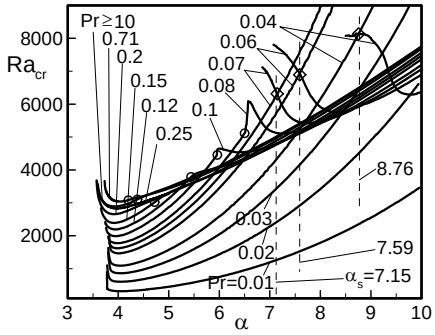

Figure 8. Variations of the critical Rayleigh number Ra_{cr} as functions of the heating wave number α for selected values of the Prandtl number Pr in the range from Pr ∈ (0.01, 1000).

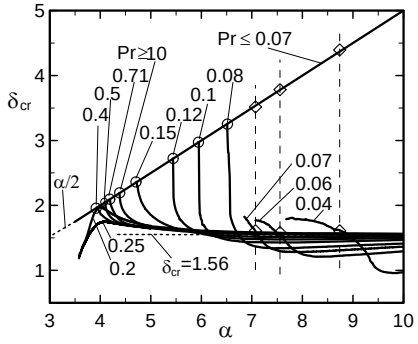

Figure 9. Variations of the critical disturbance wave number δ_{cr} as function of the heating wave number α for selected values of the Prandtl number Pr in the range from Pr ∈ (0.01, 1000).

At this point, we will discuss the case of arbitrary Prandtl number fluids. Critical stability curves for Pr varying between 0.01 and 1000 are displayed in Figs 8 and 9. We have identified four different types of responses depending on Pr of the fluid. Single, smooth critical curves exist for Pr>~0.4 , we call this as type A response where the disturbance pattern is locked-in with the heating pattern over a certain range of heating wave numbers α and there is no lock-in over the rest of the α-range. Type B occurs for Pr ∈ (~0.19, ~0.4) and also has single, smooth critical curves but its characteristic signature involves curves describing critical wave numbers δ_{cr} which turn downwards in a characteristic manner as α decreases (see Fig.9). Type C is observed for Pr ∈ (~0.08, ~0.19) and is characterized by the critical curves displaying a characteristic bump, with the size of this bump increasing and moving towards larger values of α as Pr decreases (see Fig.8). Type D is observed for Pr < ~0.08 and is characterized by the existence of two branches of the critical curve, with branch one corresponding to the locked-in pattern and branch two corresponding to the no locked-in pattern, and both patterns co-existing at a specific, Pr-depend value of α (intersection of both branches).

Conclusions

Natural, buoyancy-driven convection of a Boussinesq fluid contained in an infinite slot has been analyzed. The slot is subject to a spatially distributed heating and the gravity is directed across the slot. It is assumed that the mean temperatures of both walls are the same and thus the convection occurs only due to the spatial variability of the heating. Results are presented for the case of sinusoidal variations of temperature of the lower wall while the temperature of the upper wall is kept constant. Conditions leading to the emergence of roll instability have been identified. The system response is a strong function of the Prandtl number, especially for smaller values of Pr. In the case of moderate α the pattern of instability is generally locked-in with the pattern of heating according to the relation $\delta_{cr} = \alpha/2$. In the case of large α, the critical disturbance wave number becomes independent of α and approaches value $\delta_{cr} = 1.56$ when α is large enough. It has been shown that in this case the critical value of Ra increases proportionally to $\alpha^{1.5}$ for all values of Pr. Four different types of responses are identified depending on Pr of the fluid.

Acknowledgments

This work has been carried out with support from SHARCNET and NSERC of Canada. SHARCNET of Canada provided the computing resources.

References

[1] Bodenschatz, E., Pesh, W. & Ahlers, G., Recent developments in Rayleigh-Benard convection, *Annu. Rev. Fluid Mech.*, **32**, 2000, 709-778.

[2] Kierzenka, J. & Shampine, L.F., A BVP Solver that Controls Residual and Error. *JNAIAM*, **3**, 2008, 27-41.

[3] Lyubimov, T. P., Lyubimov, D. V., Morozov, V. A., Scuridin, R. V., Hadid, H. B. & Henry, D., Stability of convection in a horizontal channel subjected to a longitudinal temperature gradient. Part 1. Effect of aspect ratio and Prandtl number, *J . Fluid Mech.,* **635**, 2009, 275-295.

[4] Mancho, A. M., Herrero, H. & Burguete J., Primary instability in convective cells due to nonuniform heating, *Phys. Rev. E,* **56(3)**, 1997, 2916-2923

[5] Mullarney, J. C., Griffiths, R.W. & Hughes, G. O., Convection driven by differential heating at a horizontal boundary, *J. Fluid Mech.,* **516**, 2004, 181–209.

[6] Natarajan, E., Basak, T. & Roy, S., Natural convection flows in a trapezoidal enclosure with uniform and non-uniform heating of bottom wall, *Int. J. Heat Mass. Trans.,* **51**, 2008, 747-756

[7] Rossby, T., Numerical experiments with a fluid heated non-uniformly from below, *Tellus,* **50A**, 1998, 242-257.

[8] Wang, W. & Huang, R. X., An experimental study on thermal circulation driven by horizontal differential heating, *J. Fluid Mech.,* **540**, 2005, 49–73.

[9] Verzicco, R. & Camussi, R., Prandtl number effects in convective turbulence, *J. Fluid Mech.,* **383**, 1999, 55-73.